The Influence of Concentrations of Sensitizers and Activators on Luminescence Kinetics Parameters of Upconversion Nanocomplexes NaYF4:Yb3+/Tm3+

Sergey Burikov *, Ekaterina Filippova, Vera Proydakova, Sergey Kuznetsov, Valery Voronov, Natalia Tabachkova, Tatiana Dolenko

Posted Date: 9 January 2024

doi: 10.20944/preprints202401.0675.v1

Keywords: upconversion luminescence; rare earth ions; time-resolved spectroscopy; colloids

Article

The Influence of Concentrations of Sensitizers and Activators on Luminescence Kinetics Parameters of Upconversion Nanocomplexes $NaYF_4:Yb^{3+}/Tm^{3+}$

Sergey Burikov [1,*], Ekaterina Filippova [1], Vera Proydakova [2], Sergey Kuznetsov [2], Valery Voronov [2], Natalia Tabachkova [2] and Tatiana Dolenko [1]

[1] Moscow State University, Department of Physics, Russia, Moscow; sergey.burikov@gmail.com
[2] Prokhorov General Physics Institute of the Russian Academy of Sciences, Russia, Moscow; kouznetzovsv@gmail.com
* Correspondence: sergey.burikov@gmail.com

Abstract: For colloids of $NaYF_4:Yb^{3+}/Tm^{3+}$ nanoparticles in DMSO by the method of time-resolved luminescence spectroscopy with nanosecond pulsed excitation at a wavelength of 975 nm the photophysical processes that determine the course of kinetic curves have been revealed. It has been found that the luminescence rise time decreases with an increase of the concentration of activators and sensitizers due to increase of the efficiency of energy transfer from sensitizers to activators. Cross-relaxation of the excited states of activators provides a decrease of the luminescence decay time with an increase of the concentration of activators and a constant concentration of the sensitizer. There was no correlation between the time of luminescence decay with the change of the concentration of sensitizers and constant concentration of activators due to the competition of the processes of energy back transfer from activators to sensitizers and the "feeding" of activators by excitations coming from remote sensitizer ions.

Keywords: upconversion luminescence; rare earth ions; time-resolved spectroscopy; colloids

1. Introduction

Luminescent nanoparticles and dispersions based on them represent considerable interest, since when doped with rare earth elements, they exhibit intense anti-stokes (up-conversion) luminescence in the visible range of the spectrum when excited in the near IR range [1-4]. Excitation in the near-infrared range, located in the transparency region, opens up wide opportunities for biovisualization and sensorics of various processes occurring in living cells. In addition, up-conversion luminophores are used for hidden protective marking [5], in photovoltaic devices [6], as fluorescent markers and drug carriers in biomedical applications [7-9], thermosensors [10,11], in vacuum measurement [12], for increase of the efficiency of solar panels [13,14], laser cooling [15], and up-conversion lasers [16].

In order to obtain effective anti–stokes luminescence, it is necessary to dope nanoparticles with a pair of active rare earth elements, one of which has a large absorption cross-section (sensitizer), and the other has intense luminescence (activator). The sensitizer absorbs the exciting radiation and transmits the excitation to the activator. Ytterbium ions are often used as sensitizers, and thulium, erbium or holmium ions are used as activators [17-19]. Unlike nonlinear optical processes that occur by means of quasi-virtual energy levels, up-conversion occurs by means of real energy state. At the same time, various mechanisms take place: energy transfer followed by absorption from the excited state, consecutive transfer of excitation energy, cross-relaxation up-conversion, cooperative sensitization, and cooperative luminescence [20]. The scheme of the electronic levels of the sensitizer (ytterbium) and activator (thulium) and the mechanisms of excitation transmission are shown in Fig.1. One of the most effective matrices for doping are nanopowders with a crystal structure of the gagarinite type based on $NaYF_4$ [21] and $NaGdF_4$ [22].

Preprints (www.preprints.org) | NOT PEER-REVIEWED | Posted: 9 January 2024 doi:10.20944/preprints202401.0675.v1

The luminescent properties of upconversion luminophores depend on the type of crystal matrix [23,24], the intensity of exciting radiation [22,25,26], temperature [11,27] and the environment in which the emitting nanoparticles are located [28].

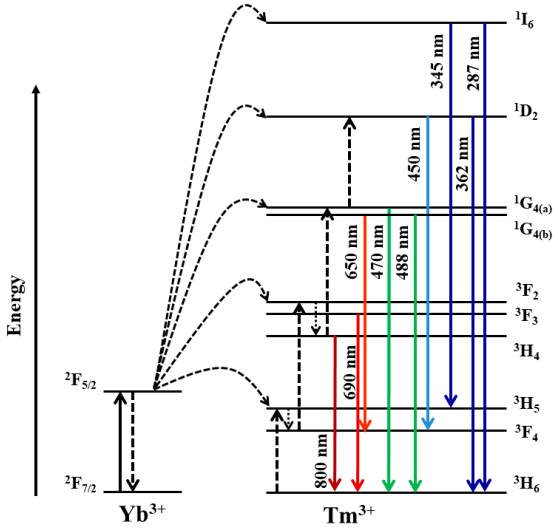

Figure 1. Diagram of the energy levels of the sensitizer (ytterbium) and activator (thulium).

Concentrations of activator and sensitizer ions also have a significant effect on the luminescence characteristics of up-conversion nanoparticles [29,30]. As concentration of the activator increases, the distance between the ions decreases. This leads to the processes of cross-relaxation and increase of the probability of transfer of excitation energy to the unexcited ion as a result of electromagnetic interaction between ions [31].

As a result, the luminescence intensity of up-conversion nanoparticles depends non-linearly on the concentration of activator ions [30], along with this there are activator concentrations at which the luminescence intensity is maximal [32,33]. An increase of the concentration of the sensitizer at a fixed concentration of the activator leads to decrease of the distance between the ions, and, as a consequence, to the increase of the efficiency of energy transfer [30].

Indirect excitation of luminescence in upconversion nanoparticles leads to the fact that the kinetic dependences of luminescence intensity under excitation by short (nanosecond) pulses have a form significantly different from similar dependences for most of conventional luminophores. In these dependences, two phases are observed – the phase of signal rise and the phase of its decay [34]. The presence of the increase phase is due to the fact that the population of the excited levels of the activator occurs gradually due to the transfer of energy from the sensitizer. As a result, the kinetic curves reflect the dynamics of two competing processes – the gradual population of the excited level of the activator and the deactivation of its excited states. The rise and decay times of luminescence are determined by a number of processes occurring in nanoparticles and depend on the number of factors: the lifetimes of the involved energy states [35], the efficiency of energy transfer between sensitizer and activator ions [36], the concentration of sensitizer and activator ions and the distance between them [36,37], the host matrix material, spectral overlap between the radiation of the sensitizer and the absorption of the activator [38-40]. The use of nanosecond pulses is promising for the realization of hyperthermia in a local volume without spreading the released heat far from the area of its excitation.

Of particular interest is determination of the effect of concentrations of activators and sensitizers on the course of kinetic curves of luminescence of nanoparticles. For yttrium oxide nanoparticles doped with erbium and ytterbium, it was demonstrated that increase of the concentration of ytterbium leads to decrease of the rise and decay times for the erbium luminescence band with maximum of about 548 nm (18240 cm^{-1}), as well as to decrease of the decay time for the erbium luminescence band with maximum of about 654 nm (15286 cm^{-1}) [41]. It was not possible to identify a definite dependence of the luminescence rise time on the ytterbium concentration for the band with

 doi:10.20944/preprints202401.0675.v1

maximum of 654 nm, however, it was found that the luminescence rise time for this band is less than for the band with maximum in the region of 548 nm. For the luminescence decay times, the situation was reversed – the luminescence decay time of the band with maximum near 654 nm turned out to be longer. The authors [42] found that increase of the erbium concentration from 1 to 6% in Y_2O_2S crystals led to decrease of the decay time of the luminescence band with maximum near 550 nm. For Gd_2O_2S, with increase of the erbium concentration from 0.1 to 2.0%, the rise time of erbium luminescence increased, and with increase of the erbium concentration from 2 to 25% decreased, while the decay time increased in the range of the Er concentration from 0.1 - 10.0% and decreased in the range of 10-25% [43]. For $NaYF_4:Yb^{3+}/Tm^{3+}$ nanoparticles at the fixed ytterbium concentration, the variation of thulium concentration in the range of 0.1-2.0% leads to decrease of the rise and decay times of thulium luminescence [44].

A review of publications allows to suggest that there is a large set of data concerning the effect of activator and sensitizer concentrations on the parameters of kinetics of luminescence of up-conversion nanoparticles, while the available data are quite contradictory. There is a big problem in conducting a comparative analysis and comparing the results of different authors obtained for luminophores of nominally the same composition. The impossibility of correct comparative analysis is caused by the fact that different authors have studied nanoluminophores of the same composition, but obtained by different synthesis methods with different chemical microimpurities, with significantly different morphology and particle sizes.

In this article, the dependences of the parameters of kinetic luminescence curves of β-$NaYF_4:Yb^{3+}/Tm^{3+}$ luminophore colloids in dimethyl sulfoxide (DMSO) on the dependence on the concentration of activator and sensitizer ions synthesized by the same synthesis method according to the same synthesis protocol from the same starting reagents were investigated. For this purpose, a series of samples were specially synthesized, differing in the concentration of only activators or only sensitizers with the remaining parameters of the nanoparticles unchanged. Kinetic curves of thulium luminescence were analyzed depending on the concentrations of activator and sensitizer ions registered under the same conditions, and the system parameters (optical pumping intensity, temperature, luminescence excitation mode) were analyzed.

2. Materials and Methods

2.1. Synthesis and characterization of the samples

Nanoparticles β-$NaYF_4:Yb^{3+}/Tm^{3+}$ were synthesized by the solvothermal synthesis technique in a high-boiling solvent according to the procedure described earlier in [45, 46]. Ytterbium, thulium and yttrium acetates (purity 99.99%, Lanhit, Russia) were added to oleic acid (pure, Chimmed, Russia) and 90% octadecene-1 (Sigma Aldrich). The reaction mixture was heated up to 130 °C with stirring in an argon atmosphere until the precipitate was completely dissolved and the corresponding oleates of ytterbium, thulium and yttrium were prepared, then water and acetic acid were removed in vacuum. NaOH and NH_4F (chemically pure, Lanhit, Russia) were dissolved in methanol (chemically extra pure, Chimmed, Russia). A mixture of NaOH and NH4F solutions was added to the reaction mixture with oleates at room temperature, then the entire mixture was heated up to 50-60°C and kept at this temperature for one hour with following methanol removing in vacuum. After removing all the methanol, the reaction mixture was heated up to 315°C followed by holding for 3 hours and then cooling to 25°C. The nanoparticle precipitate was separated from the solution by centrifugation (Eppendorf 5804 centrifuge, 6500 rpm, 5 min). The resulting nanoparticles were sequentially dispersed three times in chloroform and washed with 96% ethanol. Suspensions of nanoparticles in DMSO (chemically pure, Chimmed, Russia) were prepared with the same concentration of 1 mg/ml according to the developed protocol. 10 ml of DMSO was added to 10 mg of β-$NaYF_4$:Yb/Tm nanoparticles. The resulting suspensions were sonicated at 35 kHz for 1 hour in the ultrasonic bath "GRAD 13-35".

As a result, two series of β-NaYF4:Yb3+/Tm3+ samples were synthesized in such a way that in one of the series the concentration of the sensitizer varied at the constant concentration of the

Preprints (www.preprints.org) | NOT PEER-REVIEWED | Posted: 9 January 2024 doi:10.20944/preprints202401.0675.v1

activator, and in the other series the concentration of the activator varied at the constant concentration of the sensitizer (Table 1).

Table 1. Concentrations of sensitizer and activator ions in nanopowders β-$NaYF_4$:Yb^{3+}/Tm^{3+}.

Number of the sample	1	2	3	4	5	6	7	8
Concentration Yb, mol.%	10	14	18	22	18	18	18	18
Concentration Tm, mol. %	4	4	4	4	1	2	4	6

The morphology, particle size distribution and the presence of the crystal structure were studied using JEOL JEM-2100 transmission electron microscope (Fig.2). The presence of the crystal structure was confirmed by X-ray diffraction data on the example of samples 7 and 8 (Fig.2a and Fig.2b, respectively). The particle size distribution was determined basing on 60 particles in the ImageJ software based on typical microphotographs of samples 7 and 8 (Fig.2c,d,e,f, respectively). The average particle sizes were 21.9 ± 2.8 nm and 21.1 ± 3.1 nm for samples 7 and 8, respectively. The measured sizes converge with microphotographs at high magnification (Fig.2g and Fig.2h).

The sizes of aggregates in DMSO colloids according to DLS (Malvern Zetasizer Nano ZS) were 34.1±7.3 nm on average. Such sizes indicate that there is no significant aggregation of nanoparticles in colloids.

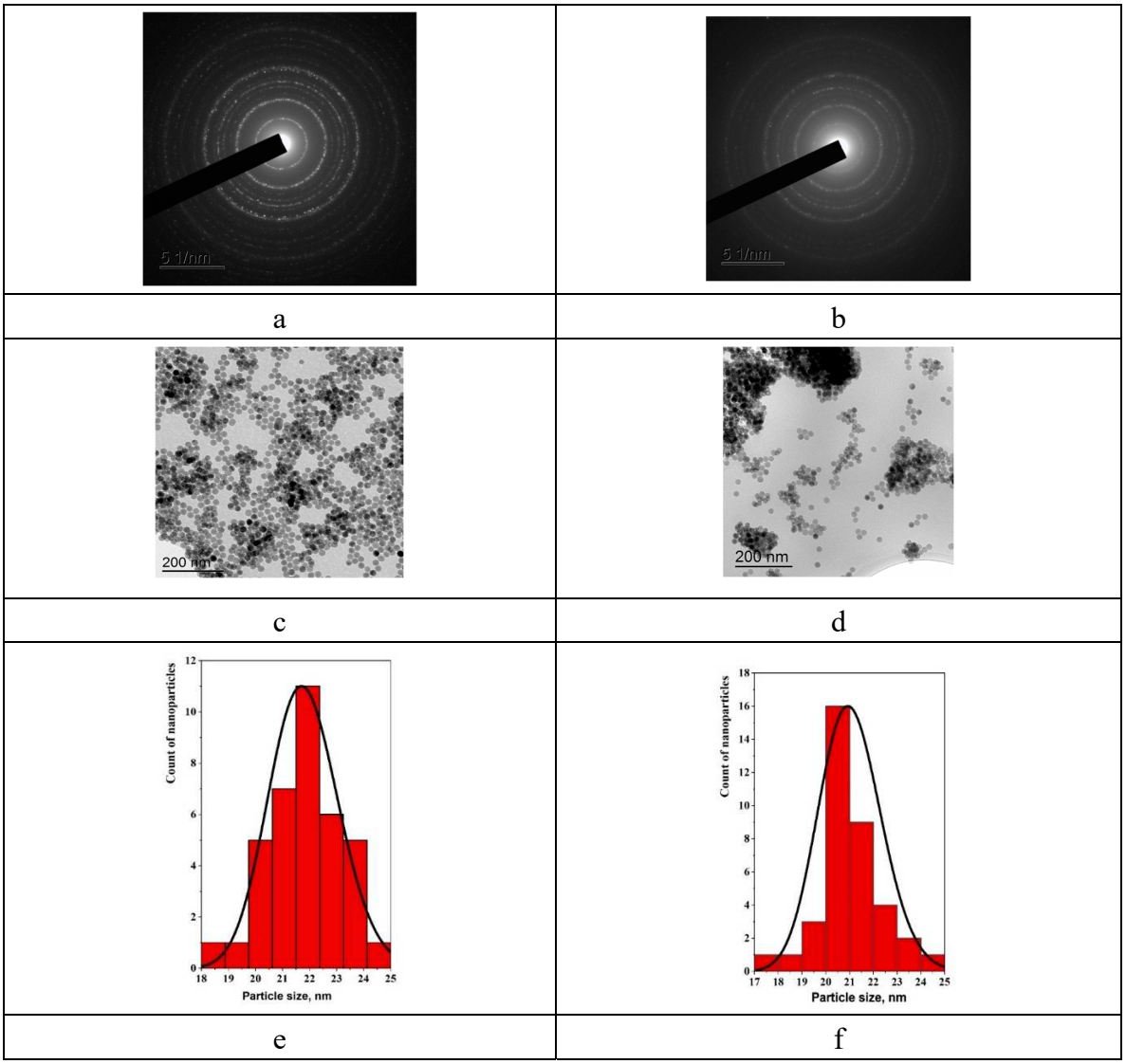

a b c d e f

Preprints (www.preprints.org) | NOT PEER-REVIEWED | Posted: 9 January 2024 doi:10.20944/preprints202401.0675.v1

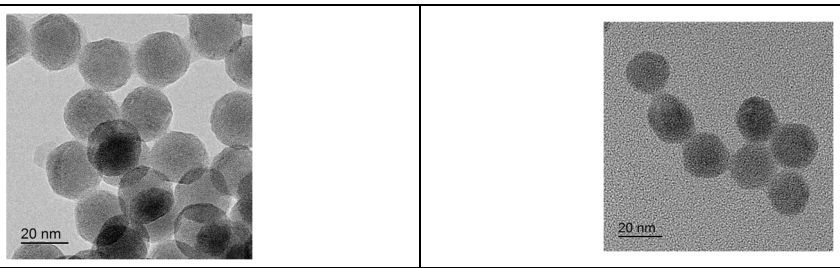

g h

Figure 2. TEM image of nanoluminophores β-$NaYF_4$: Yb^{3+}/Tm^{3+}: a – electron diffraction image for sample 7, b - electron diffraction image for sample 8, c – TEM image for sample 7, d - TEM image for sample 8, e – particle size distribution for sample 7, f – particle size distribution for sample 8, g – TEM image for sample 7 with high resolution, h - TEM image for sample 8 with high resolution.

2.2. Luminescent spectroscopy of colloids β-$NaYF_4$:Yb^{3+}/Tm^{3+} in DMSO

The Nd:YAG laser (model LQ629-100 with LP603 optical parametric oscillator (Solar, Belarus)) was used for pulsed excitation of up-conversion luminescence of β-$NaYF_4$:Yb^{3+}/Tm^{3+}. Laser power at the wavelength 975 nm was 200 mW with pulse duration of 10 ns and repetition rate 100 Hz. The peak pumping power density was about 300 MW/cm^2. The samples were probed in the 90-degree geometry of the experiment in the standard quartz cuvette (10*10*50 mm). A blocking interference filter was used to suppress the elastic scattering signal at the wavelength 975 nm.

The system of registration of luminescence spectra consisted of monochromator (MVR-80, grating 600 grooves/mm, focal length 500 mm), PMT (Hamamatsu R928) and digital oscilloscope Rigol DS1202Z-E (bandwidth 200 MHz). For registration of the luminescence spectra second detector was used – PMT Hamamatsu H-8259-1 operation in photon-counting mode.

3. Results and discussion

3.1. Investigation of the kinetics of β-$NaYF_4$:Yb^{3+}/Tm^{3+} luminescence

A typical luminescence spectrum of β-NaYF4:Yb3+/Tm3+ colloids in DMSO is shown in Fig.3.

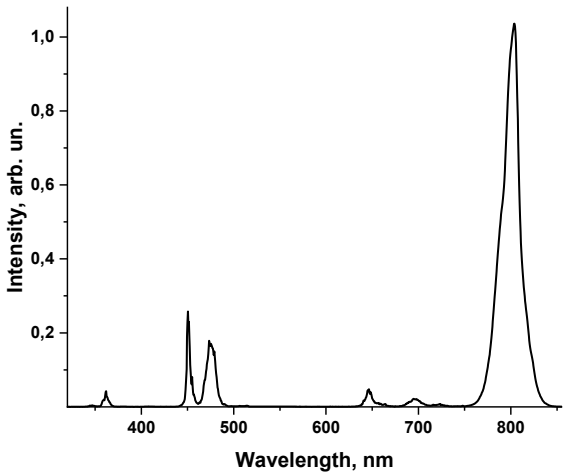

Figure 3. Luminescence spectrum of colloids β-$NaYF_4$:Yb^{3+}/Tm^{3+} nanoparticles in DMSO.

The spectrum comprises a whole set of bands with maximums at wavelengths 804, 695, 650, 476, 488, 452, 345 362 345 nm corresponding to luminescent transitions of thulium: $^3H_4 \rightarrow {}^3H_6$, $^3F_3 \rightarrow {}^3H_6$, $^1G_{4(b)} \rightarrow {}^3F_4$, $^1G_{4(a)} \rightarrow {}^3H_6$, $^1G_{4(b)} \rightarrow {}^3H_6$, $^1D_2 \rightarrow {}^3F_4$, $^1I_6 \rightarrow {}^3H_5$. Bands near 800, 450 and 475 nm are most

Preprints (www.preprints.org) | NOT PEER-REVIEWED | Posted: 9 January 2024 doi:10.20944/preprints202401.0675.v1

intensive, and it can be used for biomedical applications and biovisualization [7-10]. The band in the region of 800 nm is interesting because it is the most intense and is located in the "transparency window" of biological tissues. Luminescence bands with maximums in the region of 450 and 475 nm are thermally coupled [43] and can be used as temperature sensor [11].

Kinetic luminescence curves of above-mentioned bands were obtained for all prepared 8 β-$NaYF_4$:Yb^{3+}/Tm^{3+} colloids in DMSO. Kinetic curves for samples No. 2, 4, 6 are shown in Fig.4. Since the luminescence bands differ greatly in intensity, for the convenience of comprehension here and further, all curves are normalized to maximal intensity.

As it can be seen from the presented data, the profiles of kinetic curves differ for different bands of the luminescence spectrum. The kinetic curve for the band with a maximum in the region of 450 nm increases and decreases faster than the rest, the curve for the band in the region of 800 nm - slower than all, the curve for the band with a maximum in the region of 475 nm occupies an intermediate position.

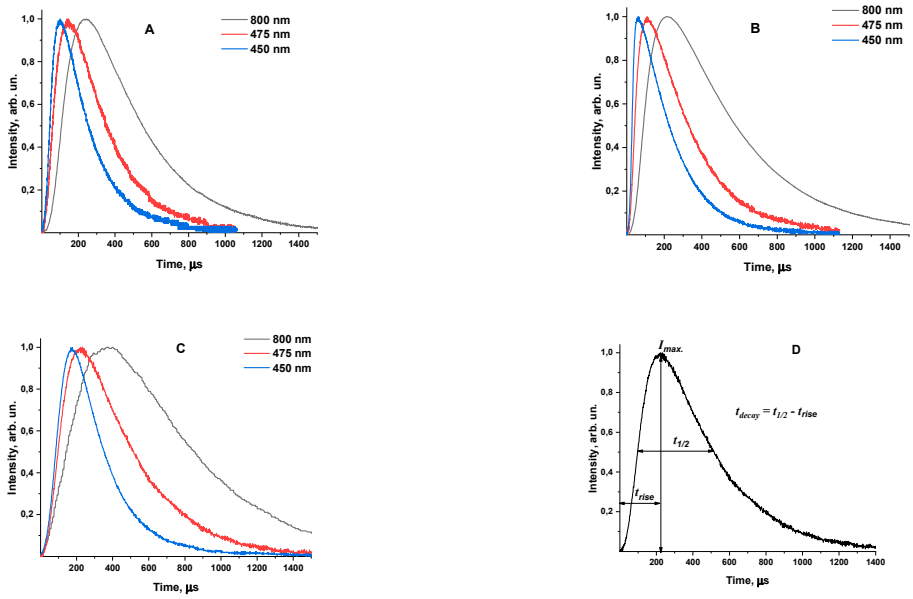

Figure 4. Kinetic curves for luminescence bands with maximum in the region of 800, 475 and 450 nm: (A) - sample 2 (Yb 14%, Tm 4%); (B) – sample 4 (Yb 22%, Tm 4%); (C) – sample 6 (Yb 18%, Tm 2%); (D) - algorithm for calculating the rise and decay time of luminescence of nanoparticles β-$NaYF_4$:Yb^{3+}/Tm^{3+}.

A similar behavior of kinetic curves for the studied luminescence bands was obtained earlier by the authors [48] for β-$NaYF_4$:20%Yb^{3+}/0.6%Tm^{3+} nanoparticles with the specified ratio of sensitizer and activator concentrations. In this study, it was found that kinetic luminescence curves behave similarly for nanoparticles with different ratios of ytterbium and thulium concentrations. For excitation of different luminescence bands, a different number of photons is required: two for the band in the region of 800 nm, three for the band in the region of 475, and four for a band in the region of 450 nm (Fig. 1). This indicates that the dominant mechanism of the formation of $NaYF_4$:20%Yb^{3+}/0.6%Tm^{3+} upconversion luminescence is nonradiative energy transfer from ytterbium ions to thulium ions. The concentration of thulium ions in the complex is always less than the concentration of ytterbium ions. Since the ions in the crystal lattice are evenly distributed, it can be assumed that one thulium ion is surrounded by several ytterbium ions. When excited by a short laser pulse, it can be assumed that after its termination, the number of ytterbium ions in the excited state is maximal and can only decrease in the future. That is, after the pump pulse is completed, the thulium ion is surrounded by ytterbium ions in the excited state. After start of excitation transfer to the thulium ion, the number of excited ytterbium ions will decrease. As a result, the probability of

 doi:10.20944/preprints202401.0675.v1

excitation of the luminescence band, which requires a large number of pumping photons, will decrease. The band around 450 nm requires 4 pumping photons, so its intensity increases and decreases the fastest. The luminescence band in the region of 800 nm requires the smallest number of pumping photons (2), so its intensity decays the slowest.

As it was established in this work, change of the concentration of ytterbium ions in the range of 10-22% or thulium in the range of 1-6% does not qualitatively change the picture. The intensity of the luminescence band requiring the largest number of pumping photons increases and decreases the fastest, and the intensity of the band requiring the smallest number of pumping photons increases and decreases the slowest.

For description of the kinetic curves two-exponential approximation model has traditionally been used [49] in the literature. Within the framework of this model, one component describes the increase in the luminescence signal and contains information about the non-radiative transfer of energy from sensitizers to activators, the other component describes the decrease of the signal and contains information about the actual decay time of the luminescence of acceptors. In our study, after analyzing all the kinetic curves, it became clear that this model poorly describes the initial section of the growth phase [48, 50, 51]. In addition, the authors [48] suggested that the transfer of energy from sensitizers to activators affects the decay time of the luminescence of activators. Moreover, when short (nanosecond) high-power laser pulses are used to excite the luminescence signal, as in our case, the intensity of excitation radiation is quite high (hundreds of MW/cm^2). In this case, in addition to energy transfer from sensitizers to activators, other mechanisms of formation of up-conversion luminescence are possible – absorption from the excited state and cooperative sensitization [1].

Since in this paper we were primarily interested in the differences in the course of curves due to different ion concentrations, and not in the description of these curves using some model, in this paper we decided not to approximate the obtained curves using some specific model. In this paper, instead of describing kinetic curves as parameters characterizing the rise and decay of luminescence, the rise time (t_{rise}) and the decay time (t_{decay}) were chosen. The rise time is the time from the moment the luminescence signal begins to rise to the moment when the luminescence signal is maximal, the decay time is the difference between the width of the kinetic curve at half the height and the rise time (Fig.4D).

3.2. Rise time of β-NaYF$_4$:Yb^{3+}/Tm^{3+} luminescence

The calculated values of the signal rise time for luminescence bands with maximums in the region of 450, 475, 800 nm for all samples are shown in Fig.5 and in Table S1.

Preprints (www.preprints.org) | NOT PEER-REVIEWED | Posted: 9 January 2024 doi:10.20944/preprints202401.0675.v1

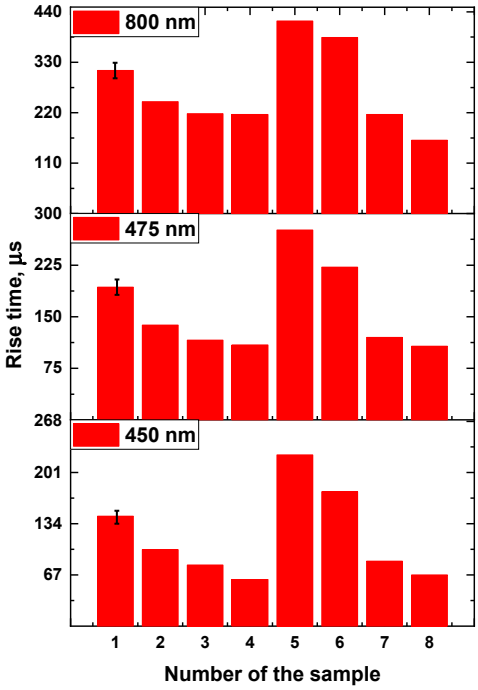

Figure 5. Rise times of luminescence signal of β-$NaYF_4$:Yb^{3+}/Tm^{3+} nanoparticles.

As it can be seen from the obtained results, increase of the concentration of ytterbium (samples 1-4) leads to decrease of the rise time of the luminescence signal for all studied bands. This is explained in terms of the effect of the concentrations of doping ions (sensitizer and activator) on the average distance between neighboring ions and, accordingly, on the luminescent properties. The efficiency of energy transfer from sensitizer ions to activator ions is determined by the distance between the sensitizer and activator ions (ion concentration) according to the formula [34,48]:

This is example 1 of an equation:

$$P = \frac{1}{t_s}\left(\frac{R_0}{R}\right)^s \quad , \tag{1}$$

where t_s is the effective lifetime of the excited state of the sensitizer ion, taking into account all channels of deactivation of the excited state, except for the energy transfer to the activator ion; R is the distance between the ions between which energy transfer occurs; R_0 is the distance between the ions at which the rate of energy transfer between the ions is equal to the rate of spontaneous decay of the excited level of the sensitizer ion; s is an index describing the multipole interaction (s=6 for dipole–dipole interaction, s=8 for dipole-quadrupole, s=10 for quadrupole-quadrupole). Increase of the concentration of sensitizer ions leads to decrease of the distance R and increases the efficiency of energy transfer to activator ions.

According to this formula (1), at the fixed concentration of thulium, an increase of the concentration of ytterbium leads to the fact that the average distance between ytterbium and thulium ions decreases and the efficiency of energy transfer from sensitizers to activators increases. As a result, the time which is necessary to reach the maximum of signal - the rise time - decreases (Fig.5, Table S1).

With the increase of the concentration of thulium (samples 5-8), the rise time of the signal also decreases (Fig.6), which can be explained similarly. At the fixed concentration of ytterbium, increase of the concentration of thulium also leads to decrease of the average distance between activators and sensitizers and increase of the efficiency of energy transfer.

In order to confirm the proposed explanations, estimates of the average distance between ions for all samples were made in the approximation of a uniform distribution of ions over the volume of

Preprints (www.preprints.org) | NOT PEER-REVIEWED | Posted: 9 January 2024 doi:10.20944/preprints202401.0675.v1

the nanoparticle. The evaluation methodology is described in more detail in Sup.Inf. It was shown in [40] that with the increase of the concentration of ytterbium from 0 to 25%, the width of the distribution of distances between ions narrows. According to the theoretical estimates of the authors [40], for $NaYF_4:Yb^{3+}/Tm^{3+}$ nanoparticles with concentration of ytterbium 25% and thulium 0.3%, the most probable distance between ytterbium and thulium ions was about 3 nm. In our work, the concentrations of ytterbium and thulium ions are quite high: 10-22% and 1-6%, respectively. As a result, it can be assumed that the distribution of distances between ions is quite narrow and it can be replaced by the average distance. The dependences of the luminescence rise times for different bands of the spectrum on the calculated average distance between ions when the concentrations of ytterbium and thulium ions change are shown in Fig. 6.

As it can be seen in Fig. 6, increase of the distance between ions leads to increase of the rise time of luminescence intensity due to decrease of the efficiency of energy transfer from sensitizers to activators.

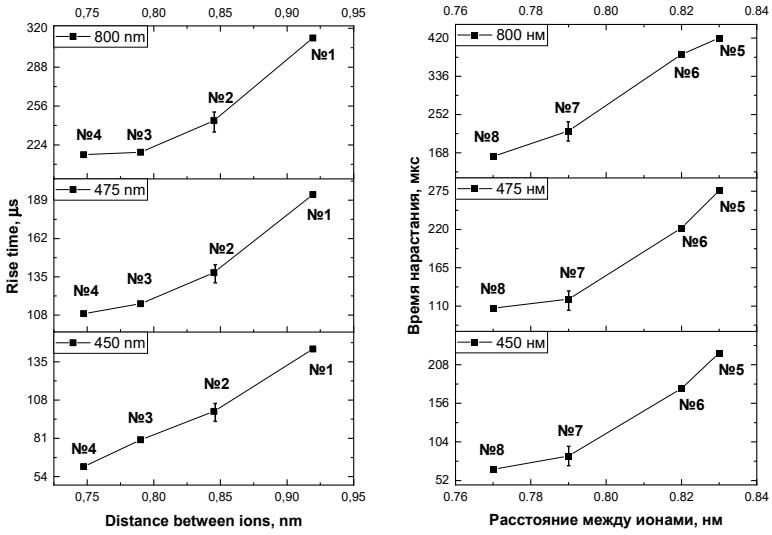

Figure 6. Dependences of the luminescence rise time on the average distance between ions for different bands of the spectrum under the change of concentration of ytterbium (left) and thulium (right).

3.3. Decay time of β-$NaYF_4:Yb^{3+}/Tm^{3+}$ luminescence

Figure 7 and Table S2 for all samples show the values of the decay time of the luminescence bands with maximums in the region of 450, 475, and 800 nm. The increase of the concentration of thulium (samples 5-8) leads to decrease of the decay time of luminescence. This can be explained by the fact that with the increase of the concentration of thulium, the probability of cross-relaxation increases [41]. As a result, this channel of excitation deactivation becomes more efficient, which leads to the decrease of time of luminescence decay.

It should be noted that in the series of samples in which the concentrations of ytterbium varied at fixed concentration of thulium (samples 1-4), there is no unambiguous tendency to increase or decrease the times of luminescence decay (Fig.7). This can be explained by the combined effect of two factors. On the one hand, the increase of the concentration of ytterbium leads to decrease of the average distance between ytterbium and thulium ions and increase of the efficiency of nonradiative energy transfer. On the other hand, the increase of the concentration of ytterbium ions increases the probability of reverse energy transfer from thulium ions to ytterbium ions [53].

Preprints (www.preprints.org) | NOT PEER-REVIEWED | Posted: 9 January 2024 doi:10.20944/preprints202401.0675.v1

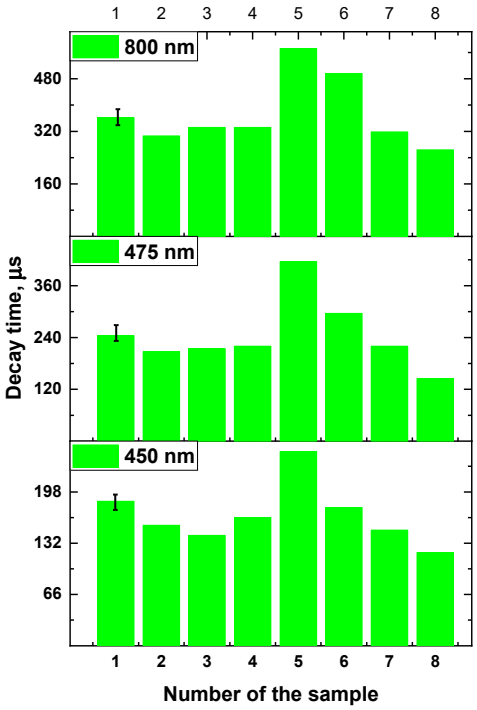

Figure 7. Luminescence decay times of the β-$NaYF_4$:Yb^{3+}/Tm^{3+} nanoparticles.

Increasing the probability of reverse energy transfer reduces the time of luminescence decay. In addition, with the increase of the concentration of ytterbium, a situation is possible in which excitation from distant ytterbium ions begins to transfer to thulium ions due to energy migration, which ensures a constant "recharge" of thulium ions with energy. This, in turn, increases the luminescence decay time. As a result, the profile of the kinetic curve is result of competition between the above-mentioned processes. Therefore, for the series of samples in which the concentrations of ytterbium varied, it is impossible to distinguish any unambiguous dependence of the luminescence decay times for all studied bands on the concentration of ytterbium.

4. Conclusions

This paper presents the results of the study of the effect of sensitizer and activator concentrations on the characteristics of luminescence kinetic curves of $NaYF_4$:Yb^{3+}/Tm^{3+} nanoparticles in DMSO obtained under nanosecond pulsed excitation.

The obtained data for two series of samples in which the concentrations of either activator or sensitizer varied showed that the characteristics of the kinetic curves of the luminescence bands of nanoparticles with maximums in the region of 450, 475, 800 nm differ over the entire range of the studied concentrations. The lowest rise and decay times of luminescence were obtained for the band with the maximum in the region of 450 nm, and the highest for the band with the maximum in the region of 800 nm. Thus, the more pumping photons are required to excite a given luminescence band, the shorter are rise and decay times of luminescence.

It was found that the rise time of the luminescence signal decreases with the increase of the concentration of both activators and sensitizers. This is due to a decrease of the average distance between ions and increase of the efficiency of energy transfer from sensitizers to activators. The decay time of the luminescence signal decreases with the increase of the concentration of activators and a constant concentration of sensitizer. The reason for this is the cross-relaxation of the excited states of the activators. A certain dependence of the luminescence attenuation time with the change of the concentration of sensitizers and the constant concentration of activators could not be established due

to the competition of the processes of energy back transfer from activators to sensitizers and the "feeding" of activators with excitations coming from remote sensitizer ions.

The results obtained in this work represent considerable interest for creation and correction of theoretical models of photophysical processes occurring in $NaYF_4:Yb^{3+}/Tm^{3+}$ complexes, as well as for control of their luminescent properties.

Supplementary Materials: The following supporting information can be downloaded at the website of this paper posted on Preprints.org, Table S1: Rise times of the luminescence signal of nanoparticles β-$NaYF_4:Yb^{3+}/Tm^{3+}$ for all samples; Table S2: Decay times of the luminescence signal of nanoparticles β-$NaYF^4:Yb^{3+}/Tm^{3+}$ for all samples; Table S3: Unit cells parameters of nanoparticles β-$NaYF_4:Yb^{3+}/Tm^{3+}$ for all samples; Table S4: The calculated distances between rare earth ions.

Author Contributions: Conceptualization: TD, SK, SB; synthesis: VP, SK; sample characterization: VV, NT, VP; spectroscopy: SB, EF; data processing: SB, EF; writing—original draft preparation: SB, TD; review and editing TD, SK. All authors have read and agreed to the published version of the manuscript.

Institutional Review Board Statement: Not applicable.

Informed Consent Statement: Not applicable.

Data Availability Statement: The data that support the findings of this study are available on request from the corresponding author.

Acknowledgments: In this section, you can acknowledge any support given which is not covered by the author contribution or funding sections. This may include administrative and technical support, or donations in kind (e.g., materials used for experiments).

Conflicts of Interest: The authors declare no conflicts of interest.

References

1. Auzel, F. Upconversion and Anti-Stokes Processes with f and d Ions in Solids. *Chem. Rev.*, **2003**, *104*, 139–174. https://doi.org/10.1021/cr020357g.
2. Bloembergen, N. Solid State Infrared Quantum Counters. *Phys. Rev. Lett.*, **1959**, *2*, 84–85. https://doi.org/10.1103/physrevlett.2.84.
3. Ovsyankin, V.V.; Feofilov P.P. Mechanism of Summation of Electronic Excitations in Activated Crystals. *JETP Lett.*, **1966**, *3*, 322.
4. Salley, G. M.; Valiente, R.; Guedel, H. U. Luminescence Upconversion Mechanisms in Yb3+–Tb3+ Systems. *J. Lumin.*, **2001**, *94–95*, 305–309. https://doi.org/10.1016/s0022-2313(01)00310-6.
5. You, M.; Zhong, J.; Hong, Y.; Duan, Z.; Lin, M.; Xu, F. Inkjet Printing of Upconversion Nanoparticles for Anti-Counterfeit Applications. *Nanoscale*, **2015**, *7*, 4423–4431. https://doi.org/10.1039/c4nr06944g
6. Han, S.; Deng, R.; Xie, X.; Liu, X. Enhancing Luminescence in Lanthanide-Doped Upconversion Nanoparticles. *Angew. Chem. Int. Ed.*, **2014**, *53*, 11702–11715. https://doi.org/10.1002/anie.201403408
7. Escudero, A.; Becerro, A. I.; Carrillo-Carrión, C.; Núñez, N. O.; Zyuzin, M. V.; Laguna, M.; González-Mancebo, D.; Ocaña, M.; Parak, W. J. Rare Earth Based Nanostructured Materials: Synthesis, Functionalization, Properties and Bioimaging and Biosensing Applications. *Nanophotonics*, **2017**, *6*, 881–921. https://doi.org/10.1515/nanoph-2017-0007.
8. Liang, G.; Wang, H.; Shi, H.; Wang, H.; Zhu, M.; Jing, A.; Li, J.; Li, G. Recent Progress in the Development of Upconversion Nanomaterials in Bioimaging and Disease Treatment. *Journal of Nanobiotechnology*, **2020**, *18*, 154. https://doi.org/10.1186/s12951-020-00713-3.
9. Reddy, K. L.; Rai, M.; Prabhakar, N.; Arppe, R.; Rai, S. B.; Singh, S. K.; Rosenholm, J. M.; Krishnan, V. Controlled Synthesis, Bioimaging and Toxicity Assessments in Strong Red Emitting Mn2+ Doped NaYF4:Yb3+/Ho3+ Nanophosphors. *RSC Adv.*, **2016**, *6*, 53698–53704. https://doi.org/10.1039/c6ra07106f.
10. Jaque, D.; Vetrone, F. Luminescence Nanothermometry. *Nanoscale*, **2012**, *4*, 4301. https://doi.org/10.1039/c2nr30764b.
11. Sarmanova, O. E.; Burikov, S. A.; Laptinskiy, K. A.; Kotova, O. D.; Filippova, E. A.; Dolenko, T. A. In Vitro Temperature Sensing with Up-Conversion NaYF4:Yb3+/Tm3+-Based Nanocomposites: Peculiarities and Pitfalls. *Spectrochim. Acta A*, **2020**, *241*, 118627. https://doi.org/10.1016/j.saa.2020.118627.
12. Runowski, M.; Woźny, P.; Lis, S.; Lavín, V.; Martín, I. R. Optical Vacuum Sensor Based on Lanthanide Upconversion—Luminescence Thermometry as a Tool for Ultralow Pressure Sensing. *Adv. Mater. Technol*, **2020**, *5*, 1901091. https://doi.org/10.1002/admt.201901091.
13. Singh, R.; Madirov, E.; Busko, D.; Hossain, I. M.; Konyushkin, V. A.; Nakladov, A. N.; Kuznetsov, S. V.; Farooq, A.; Gharibzadeh, S.; Paetzold, U. W.; et al. Harvesting Sub-Bandgap Photons via Upconversion for

Perovskite Solar Cells. *ACS Appl. Mater. Interfaces*, **2021**, *13*, 54874–54883. https://doi.org/10.1021/acsami.1c13477.

14. Karimov, D. N.; Demina, P. A.; Koshelev, A. V.; Rocheva, V. V.; Sokovikov, A. V.; Generalova, A. N.; Zubov, V. P.; Khaydukov, E. V.; Koval'chuk, M. V.; Panchenko, V. Ya. Upconversion Nanoparticles: Synthesis, Photoluminescence Properties, and Applications. *Nanotechnol Russ.*, **2020**, *15*, 655–678. https://doi.org/10.1134/s1995078020060117.
15. Dobretsova, E. A.; Xia, X.; Pant, A.; Lim, M. B.; De Siena, M. C.; Boldyrev, K. N.; Molchanova, A. D.; Novikova, N. N.; Klimin, S. A.; Popova, M. N.; et al. Hydrothermal Synthesis of Yb3+: LuLiF4 Microcrystals and Laser Refrigeration of Yb3+: LuLiF4/Silicon-Nitride Composite Nanostructures. *Laser Photonics Rev.*, **2021**, *15*, 2100019 https://doi.org/10.1002/lpor.202100019.
16. Scheps, R. Upconversion Laser Processes. *Prog. Quantum. Electron.*, **1996**, *20*, 271–358. https://doi.org/10.1016/0079-6727(95)00007-0.
17. Chen, G.; Ohulchanskyy, T. Y.; Kumar, R.; Ågren, H.; Prasad, P. N. Ultrasmall Monodisperse NaYF4:Yb3+/Tm3+ Nanocrystals with Enhanced Near-Infrared to Near-Infrared Upconversion Photoluminescence. *ACS Nano*, **2010**, *4*, 3163–3168. https://doi.org/10.1021/nn100457j.
18. Sun, Y.; Chen, Y.; Tian, L.; Yu, Y.; Kong, X.; Zhao, J.; Zhang, H. Controlled Synthesis and Morphology Dependent Upconversion Luminescence of NaYF4:Yb, Er Nanocrystals. *Nanotechnology*, **2007**, *18*, 275609. https://doi.org/10.1088/0957-4484/18/27/275609.
19. Krämer, K. W.; Biner, D.; Frei, G.; Güdel, H. U.; Hehlen, M. P.; Lüthi, S. R. Hexagonal Sodium Yttrium Fluoride Based Green and Blue Emitting Upconversion Phosphors. *Chem. Mater.*, **2004**, *16*, 1244–1251. https://doi.org/10.1021/cm031124o.
20. Zhou, J.; Liu, Q.; Feng, W.; Sun, Y.; Li, F. Upconversion Luminescent Materials: Advances and Applications. *Chem. Rev.*, **2014**, *115*, 395–465. https://doi.org/10.1021/cr400478f.
21. Hu, Y.; Sun, Y.; Li, Y.; Sun, S.; Huo, J.; Zhao, X. A Facile Synthesis of NaYF4:Yb3+/Er3+Nanoparticles with Tunable Multicolor Upconversion Luminescence Properties for Cell Imaging. *RSC Adv.*, **2014**, *4*, 43653–43660. https://doi.org/10.1039/c4ra05205f.
22. Kormshchikov, I. D.; Voronov, V. V.; Burikov, S. A.; Dolenko, T. A.; Kuznetsov, S. V. Study of Stability of Luminescence Intensity of B-NaGdF4:Yb:Er Nanoparticle Colloids in Aqueous Solution. *Nanosyst.: Phys. Chem. Math.*, **2021**, *12*, 218–223. https://doi.org/10.17586/2220-8054-2021-12-2-218-223.
23. Bazhukova, I. N.; Pustovarov, V. A.; Myshkina, A. V.; Ulitko, M. V. Luminescent Nanomaterials Doped with Rare Earth Ions and Prospects for Their Biomedical Applications (A Review). *Opt Spectrosc*, **2020**, *128*, 2050–2068. https://doi.org/10.1134/s0030400x20120875.
24. Kuznetsov, S.; Ermakova, Yu.; Voronov, V.; Fedorov, P.; Busko, D.; Howard, I. A.; Richards, B. S.; Turshatov, A. Up-Conversion Quantum Yields of SrF2:Yb3+,Er3+ Sub-Micron Particles Prepared by Precipitation from Aqueous Solution. *J. Mater. Chem. C*, **2018**, *6*, 598–604. https://doi.org/10.1039/c7tc04913g.
25. Pollnau, M.; Gamelin, D. R.; Lüthi, S. R.; Güdel, H. U.; Hehlen, M. P. Power Dependence of Upconversion Luminescence in Lanthanide and Transition-Metal-Ion Systems. *Phys. Rev. B*, **2000**, *61*, 3337–3346. https://doi.org/10.1103/physrevb.61.3337.
26. Burikov S.A.; Filippova E.A.; Fedyanina A.A.; Kuznetsov S.V.; Proydakova V. Yu.; Voronov V.V.; Dolenko T.A. Influence of the Intensity of Exciting Radiation on the Luminescent Properties of Nanopowders NaYF-=SUB=-4-=/SUB=- : Yb/Tm. *Opt Spectrosc*, **2022**, *130*, 655. https://doi.org/10.21883/eos.2022.06.54700.38-22.
27. Zhang, B.; Guo, X.; Zhang, Z.; Fu, Z.; Zheng, H. Luminescence Thermometry with Rare Earth Doped Nanoparticles: Status and Challenges. *J. Lumin.*, **2022**, *250*, 119110. https://doi.org/10.1016/j.jlumin.2022.119110.
28. Cong, T.; Ding, Y.; Xin, S.; Hong, X.; Zhang, H.; Liu, Y. Solvent-Induced Luminescence Variation of Upconversion Nanoparticles. *Langmuir*, **2016**, *32*, 13200–13206. https://doi.org/10.1021/acs.langmuir.6b03593.
29. Rozhnova, Yu. A.; Kuznetsov, S. V.; Luginina, A. A.; Voronov, V. V.; Ryabova, A. V.; Pominova, D. V.; Ermakov, R. P.; Usachev, V. A.; Kononenko, N. E.; Baranchikov, A. E.; et al. New Sr1−x−zRx(NH4)zF2+x−z (R = Yb, Er) Solid Solution as Precursor for High Efficiency up-Conversion Luminophor and Optical Ceramics on the Base of Strontium Fluoride. *Mater. Chem. Phys.*, **2016**, *172*, 150–157. https://doi.org/10.1016/j.matchemphys.2016.01.055.
30. Kuznetsov, S. V.; Burikov, S. A.; Fedyanina, A. A.; Filippova, E. A.; Proydakova, V. Yu.; Voronov, V. V.; Tabachkova, N. Yu.; Fedorov, P. P.; Dolenko, T. A. Impact of Sensitizer Yb and Activator Tm on Luminescence Intensity of Beta-$NaYF_4$:Yb/Tm Nanoluminophores. *Nanosyst.: Phys. Chem. Math.*, **2022**, *13*, 331–341. https://doi.org/10.17586/2220-8054-2022-13-3-331-341.
31. Pisarenko, V.F. Rare-earth scandoborates as new laser materials. *Soros. Obrazovat. Zh.* (in Rus.), **1996**, *11*, 111–116.
32. Pilch, A.; Wawrzyńczyk, D.; Kurnatowska, M.; Czaban, B.; Samoć, M.; Strek, W.; Bednarkiewicz, A. The Concentration Dependent Up-Conversion Luminescence of Ho^{3+} and Yb^{3+} Co-Doped β-$NaYF_4$. *J. Lumin.*, **2017**, *182*, 114–122. https://doi.org/10.1016/j.jlumin.2016.10.016.

33. Wei, W.; Zhang, Y.; Chen, R.; Goggi, J.; Ren, N.; Huang, L.; Bhakoo, K. K.; Sun, H.; Tan, T. T. Y. Cross Relaxation Induced Pure Red Upconversion in Activator- and Sensitizer-Rich Lanthanide Nanoparticles. *Chem. Mater.*, **2014**, *26*, 5183–5186. https://doi.org/10.1021/cm5022382.
34. Kong, J.; Shang, X.; Zheng, W.; Chen, X.; Tu, D.; Wang, M.; Song, J.; Qu, J. Revisiting the Luminescence Decay Kinetics of Energy Transfer Upconversion. *J. Phys. Chem. Lett.*, **2020**, *11*, 3672–3680. https://doi.org/10.1021/acs.jpclett.0c00619.
35. Gamelin, D. R.; Gudel, H. U. Upconversion Processes in Transition Metal and Rare Earth Metal Systems. In *Transition Metal and Rare Earth Compounds*, Hartmut Yersin; Publisher: Springer Berlin, Heidelberg, **2000**, pp. 1–56. https://doi.org/10.1007/3-540-44474-2_1.
36. Liu, H.; Jayakumar, M. K. G.; Huang, K.; Wang, Z.; Zheng, X.; Ågren, H.; Zhang, Y. Phase Angle Encoded Upconversion Luminescent Nanocrystals for Multiplexing Applications. *Nanoscale*, **2017**, *9*, 1676–1686. https://doi.org/10.1039/c6nr09349c.
37. Naccache, R.; Vetrone, F.; Speghini, A.; Bettinelli, M.; Capobianco, J. A. Cross-Relaxation and Upconversion Processes in Pr3+ Singly Doped and Pr3+/Yb3+ Codoped Nanocrystalline Gd3Ga5O12: The Sensitizer/Activator Relationship. *J. Phys. Chem. C*, **2008**, *112*, 7750–7756. https://doi.org/10.1021/jp711494d.
38. Dexter, D. L. A Theory of Sensitized Luminescence in Solids. *J. Chem. Phys.*, **1953**, *21*, 836–850. https://doi.org/10.1063/1.1699044.
39. Nadort, A.; Zhao, J.; Goldys, E. M. Lanthanide Upconversion Luminescence at the Nanoscale: Fundamentals and Optical Properties. *Nanoscale*, **2016**, *8*, 13099–13130. https://doi.org/10.1039/c5nr08477f.
40. Villanueva-Delgado, P.; Krämer, K. W.; Valiente, R. Simulating Energy Transfer and Upconversion in β-NaYF4: Yb3+, Tm3+. *J. Phys. Chem. C*, **2015**, *119*, 23648–23657. https://doi.org/10.1021/acs.jpcc.5b06770.
41. Hong-Wei, S.; Hai-Ping, X.; Bao-Juan, S.; Shao-Zhe, L.; Zhong-Xin, L.; Li-Xin, Y. Upconversion Luminescence Dynamics in Er 3+ /Yb 3+ Codoped Nanocrystalline Yttria. *Chin. Phys. Lett.*, **2006**, *23*, 474–477. https://doi.org/10.1088/0256-307x/23/2/056.
42. Chen, X. Y.; Zhuang, H. Z.; Liu, G. K.; Li, S.; Niedbala, R. S. Confinement on Energy Transfer between Luminescent Centers in Nanocrystals. *J. Appl. Phys.*, **2003**, *94*, 5559–5565. https://doi.org/10.1063/1.1614865.
43. Martín-Rodríguez, R.; Rabouw, F. T.; Trevisani, M.; Bettinelli, M.; Meijerink, A. Upconversion Dynamics in Er3+-Doped Gd2O2S: Influence of Excitation Power, Er3+ Concentration, and Defects. *Adv. Opt. Mater.*, **2015**, *3*, 558–567. https://doi.org/10.1002/adom.201400588.
44. Misiak, M.; Prorok, K.; Cichy, B.; Bednarkiewicz, A.; Stręk, W. Thulium Concentration Quenching in the Up-Converting α-Tm3+/Yb3+ NaYF4 Colloidal Nanocrystals. *Opt. Mater.*, **2013**, *35*, 1124–1128. https://doi.org/10.1016/j.optmat.2013.01.002.
45. Pominova, D.; Proydakova, V.; Romanishkin, I.; Ryabova, A.; Kuznetsov, S.; Uvarov, O.; Fedorov, P.; Loschenov, V. Temperature Sensing in the Short-Wave Infrared Spectral Region Using Core-Shell $NaGdF_4$:Yb^{3+}, Ho^{3+}, Er^{3+}@$NaYF_4$ Nanothermometers. *Nanomaterials*, **2020**, *10*, 1992. https://doi.org/10.3390/nano10101992.
46. Liu, J.; Chen, G.; Hao, S.; Yang, C. Sub-6 Nm Monodisperse Hexagonal Core/Shell NaGdF4Nanocrystals with Enhanced Upconversion Photoluminescence. *Nanoscale*, **2017**, *9*, 91–98. https://doi.org/10.1039/c6nr08675f.
47. Wade, S. A.; Collins, S. F.; Baxter, G. W. Fluorescence Intensity Ratio Technique for Optical Fiber Point Temperature Sensing. *J. Appl. Phys.*, **2003**, *94*, 4743–4756. https://doi.org/10.1063/1.1606526.
48. Alyatkin, S.; Asharchuk, I.; Khaydukov, K.; Nechaev, A.; Lebedev, O.; Vainer, Y.; Semchishen, V.; Khaydukov, E. The Influence of Energy Migration on Luminescence Kinetics Parameters in Upconversion Nanoparticles. *Nanotechnology*, **2016**, *28*, 035401. https://doi.org/10.1088/1361-6528/28/3/035401.
49. Buisson, R.; Vial, J. C. Transfer inside Pairs of Pr3+ in LaF3 Studied by Up-Conversion Fluorescence. *Journal de Physique Lettres*, **1981**, *42*, 115–118. https://doi.org/10.1051/jphyslet:01981004205011500.
50. Mikheev, A. V.; Kazakov, B. N. Rise Kinetics of Up-Conversion Luminescence under Pulsed Excitation. Probabilistic Model and Experiment. *J. Lumin.*, **2019**, *205*, 167–178. https://doi.org/10.1016/j.jlumin.2018.08.081.
51. Mikheev, A. V.; Kazakov, B. N. Rise Kinetics of Up-Conversion Luminescence of the LiY0.8Yb0.2F4:Tm3+ (0.2 at %) Crystal with Pulsed Excitation. *Phys. Solid State*, **2019**, *61*, 860–866. https://doi.org/10.1134/s1063783419050172.
52. Clegg, R. M. Chapter 1 Förster Resonance Energy Transfer—FRET What Is It, Why Do It, and How It's Done. *Fret and Flim Techniques*, **2009**, 1–57. https://doi.org/10.1016/s0075-7535(08)00001-6.
53. Lemmetyinen, H.; Tkachenko, N. V.; Valeur, B.; Hotta, J.; Ameloot, M.; Ernsting, N. P.; Gustavsson, T.; Boens, N. Time-Resolved Fluorescence Methods (IUPAC Technical Report). *Pure Appl. Chem.*, **2014**, *86*, 1969–1998. https://doi.org/10.1515/pac-2013-0912.

 doi:10.20944/preprints202401.0675.v1

disclaim responsibility for any injury to people or property resulting from any ideas, methods, instructions or products referred to in the content.